Figure S1. **PET-derived receptor densities versus RNAseq gene expression |** The analysis in Fig. 1 of the main text were repeated using RNAseq data instead of microarray gene expression [47]. Yellow scatter plots indicate significant ($p_{spin} < 0.05$) and large ($r > 0.5$) expression-density correspondence. Receptor density and gene expression is z-scored.
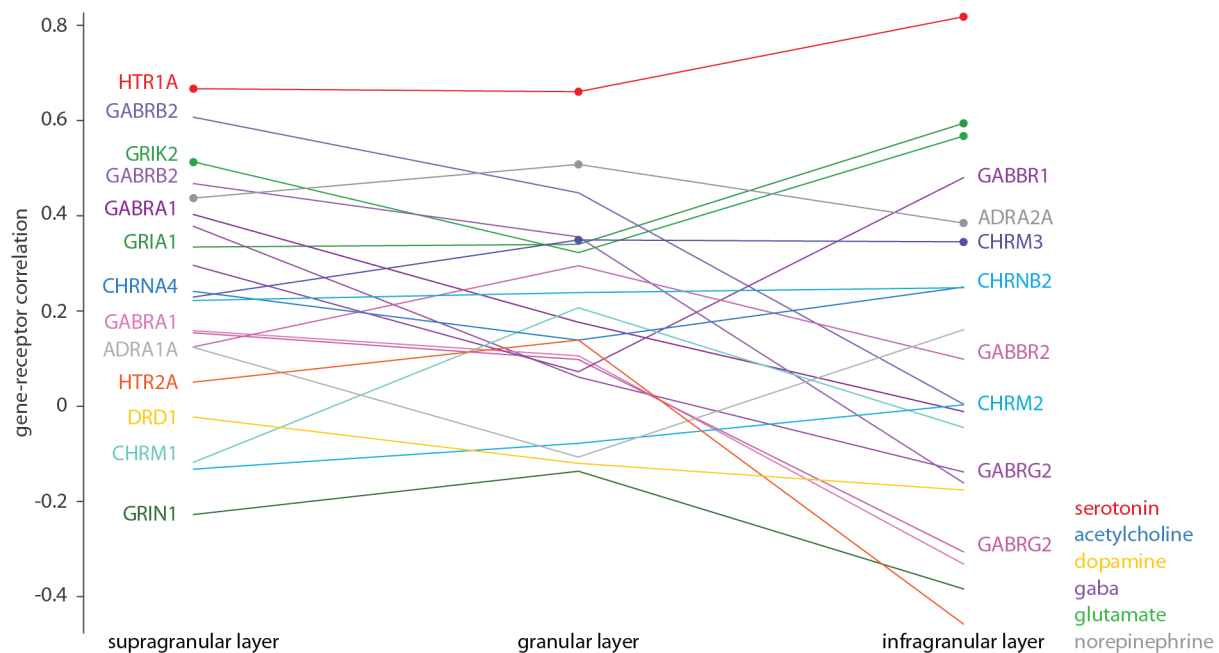
Figure S2. **Gene-receptor correlations in different laminar layers |** Gene-receptor Spearman correlation coefficients are shown in supragranular, granular, and infragranular laminar layers. Receptor density data is acquired from autoradiography [117]. Each line is associated with a gene (gene name either on the right or left of the line). Neurotransmitter systems are colour-coded according to the legend, and points refer to significant Spearman correlations ($p_{\text{spin}} < 0.05$).
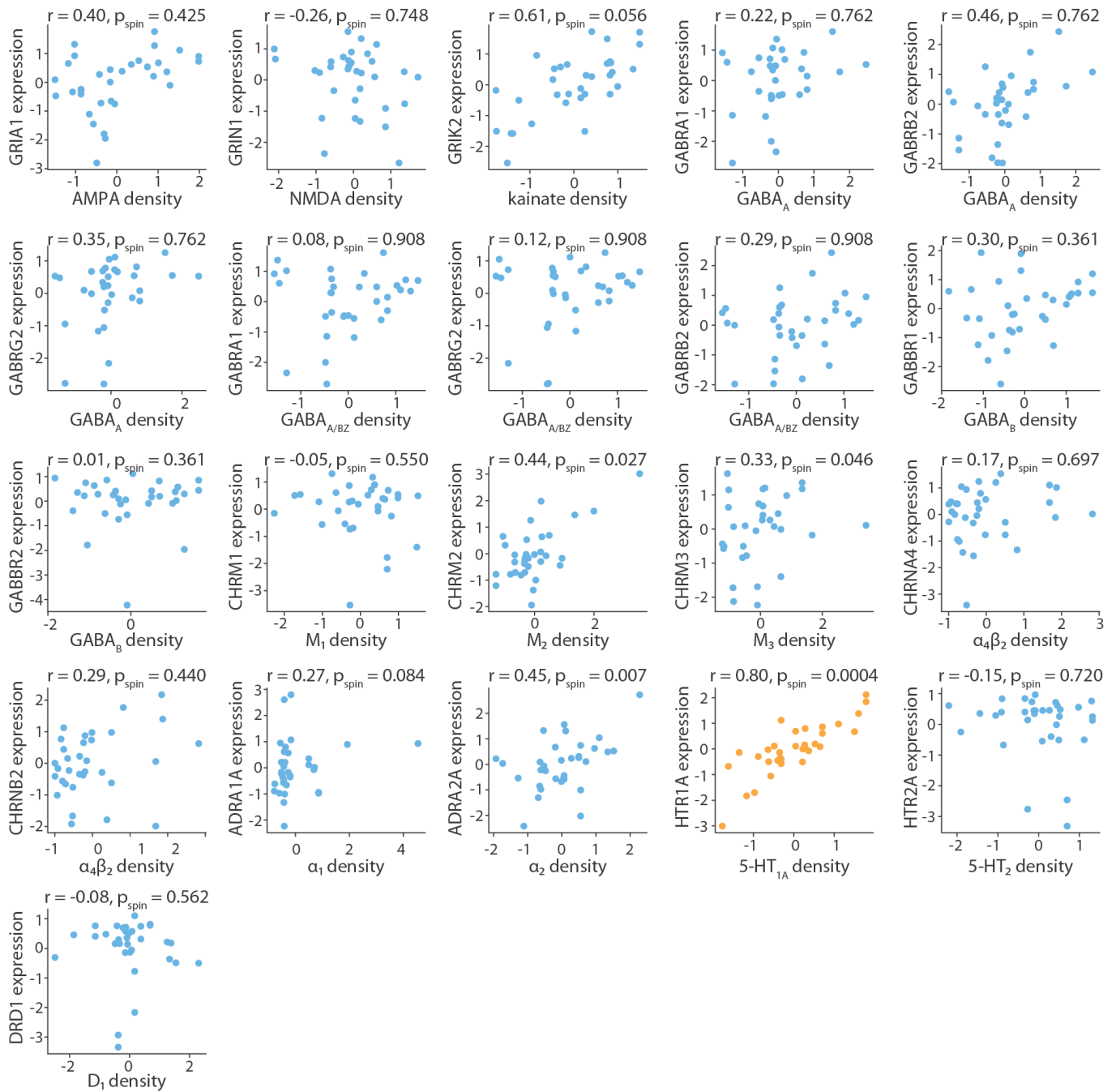
Figure S3. **Autoradiography-derived receptor densities versus RNAseq gene expression |** The analysis in Fig. 2 of the main text were repeated using RNAseq data instead of microarray gene expression [47]. Yellow scatter plots indicate significant ($p_{spin} < 0.05$) and large ($r > 0.5$) expression-density correspondence. Receptor density and gene expression is z-scored.
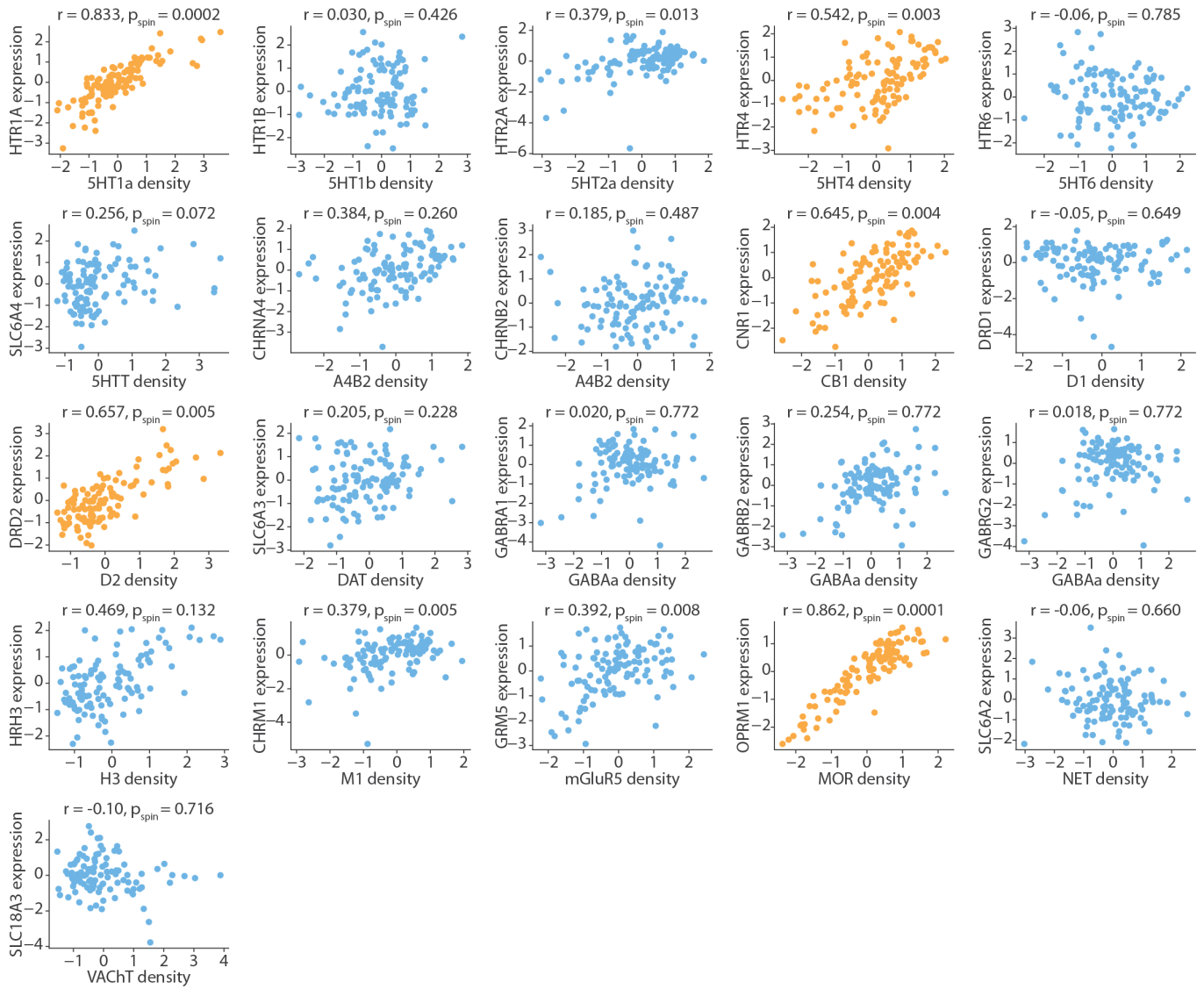
Figure S4. **Replication in a 111-node parcellation |** PET receptor/transporter densities and gene expression levels were parcellated into a 111-node cortical left hemisphere parcellation. Yellow scatter plots indicate significant ($p_{spin} < 0.05$) and large ($r > 0.5$) expression-density correspondence. Receptor density and gene expression is z-scored.
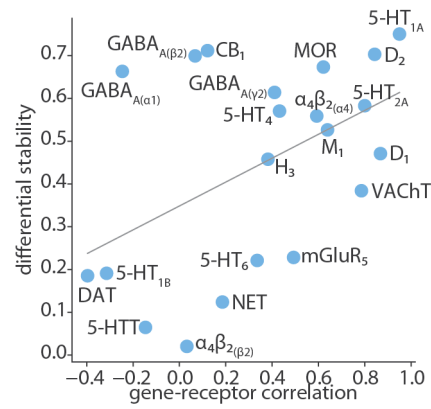
Figure S5. **Relationship between receptor expression-density correlation and differential stability in the subcortex |** We repeat Fig. 4 in the main text using the correlation between receptor gene expression and PET-derived protein density in the subcortex ($r = 0.46$, $p = 0.038$). Notably, expression-density relationships for some receptors (e.g. VAChT, D_1, and 5-HT$_6$) considerably improve in the subcortex despite low differential stability. This may be due to a smaller distance between mRNA transcripts and protein expression on the cell surface, or differences in PET radioligand binding in subcortex versus cortex (as is the case for D_1 which shows improved binding specificity in the subcortex [34]).
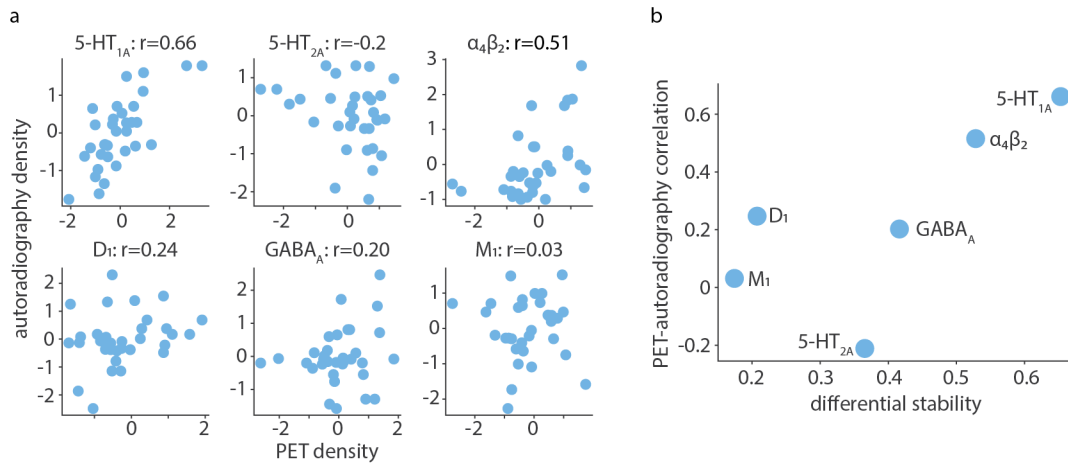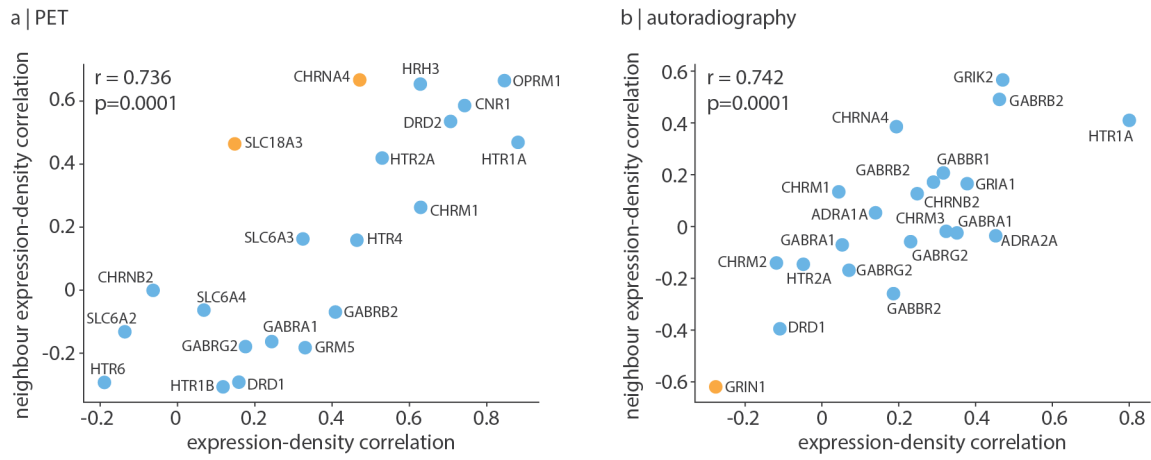

Figure S6. **Correspondence between PET- and autoradiography-derived receptor density |** (a) Spearman correlation between PET- and autoradiography-derived receptor density for the six receptors with both measurements. (b) The relationship between genetic differential stability and the PET-autoradiography correspondence for the same six receptors.

Figure S7. **Correspondence between regional receptor density and neighbouring gene expression |** For each gene-receptor pair, we correlate regional receptor density with the mean gene expression of structurally-connected neighbours, weighted by the structural connection (x-axis). Yellow points indicate significant (two-tailed $p_{\text{spin}} < 0.05$) correlations between regional receptor density and neighbouring gene expression. Next, we plot the region-neighbour correlation against the original correlation between gene expression and receptor density. This analysis was conducted using (a) PET-derived receptor density and (b) autoradiography-derived receptor density.
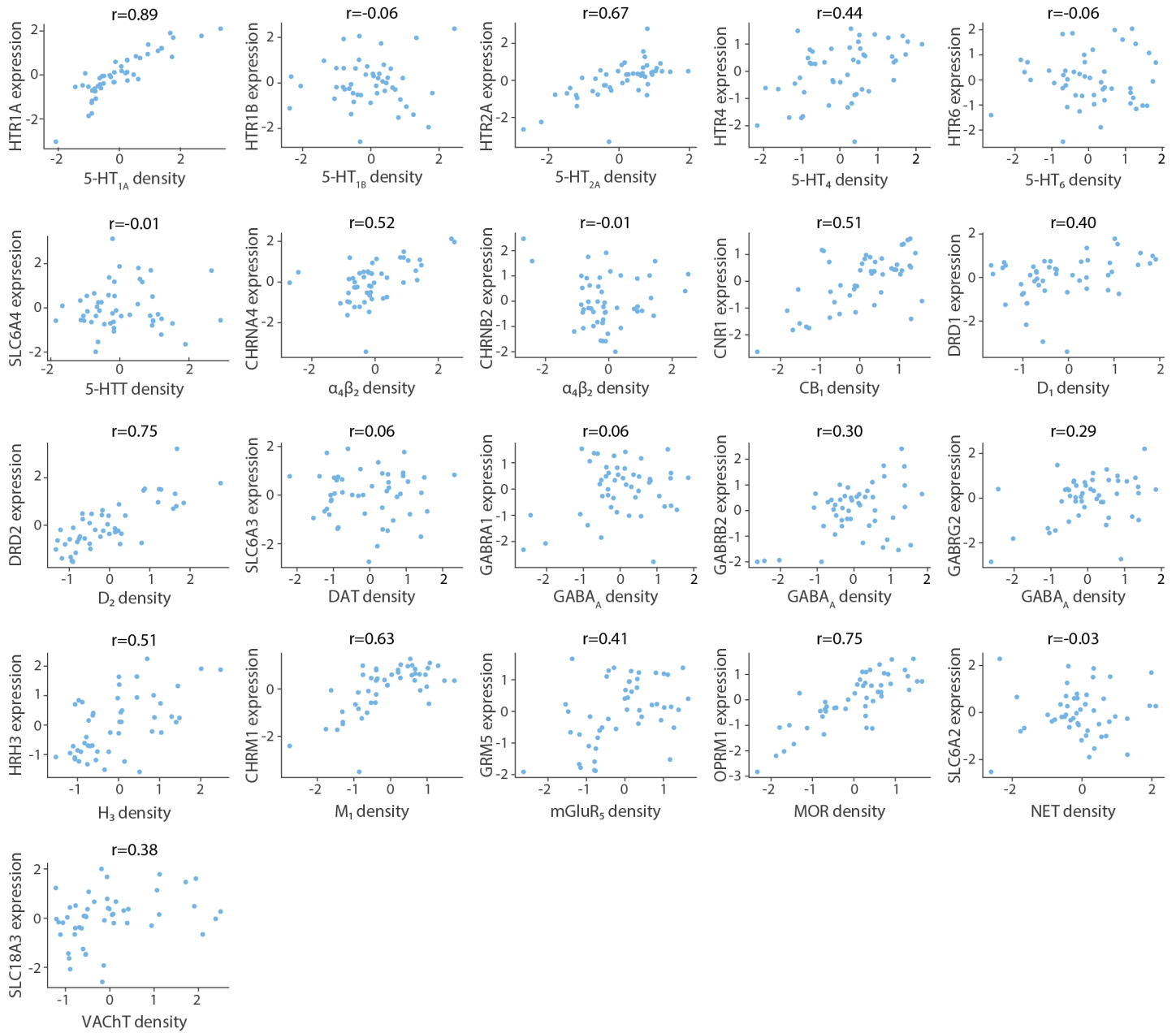
Figure S8. **PET-derived whole-brain expression-density correspondence |** For each gene-receptor pair, we separately z-score cortical and subcortical gene expression and receptor density. Then, we combine all regions into a single analysis and compare whole-brain gene expression to receptor density.
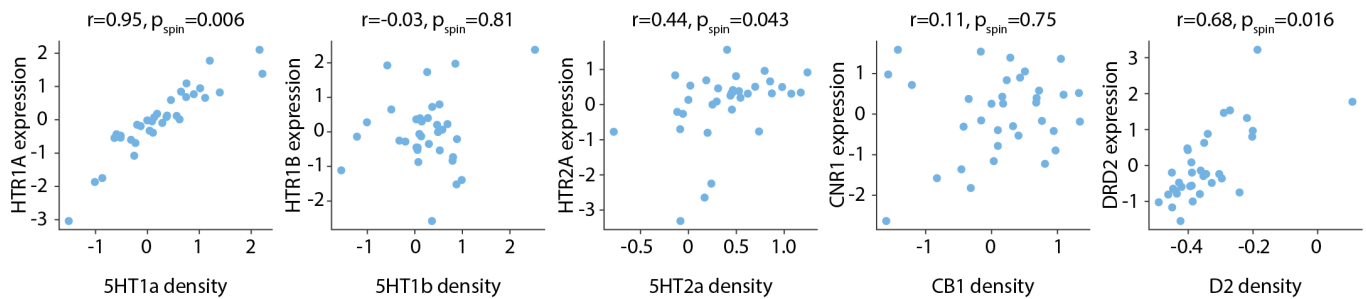
Figure S9. **Alternative PET tracer choices |** For completeness, we repeat the analysis using alternative PET tracers, which is available for five receptors: 5-HT$_{1A}$ ([^{11}C]CUMI-101 [11]), 5-HT$_{1B}$ ([^{11}C]AZ10419369 [11]), 5-HT$_{2A}$ ([^{18}F]altanserin [94]), CB$_1$ ([^{18}F]FMPEP-D2 [59]), and D$_2$ ([^{18}F]fallypride [51]).
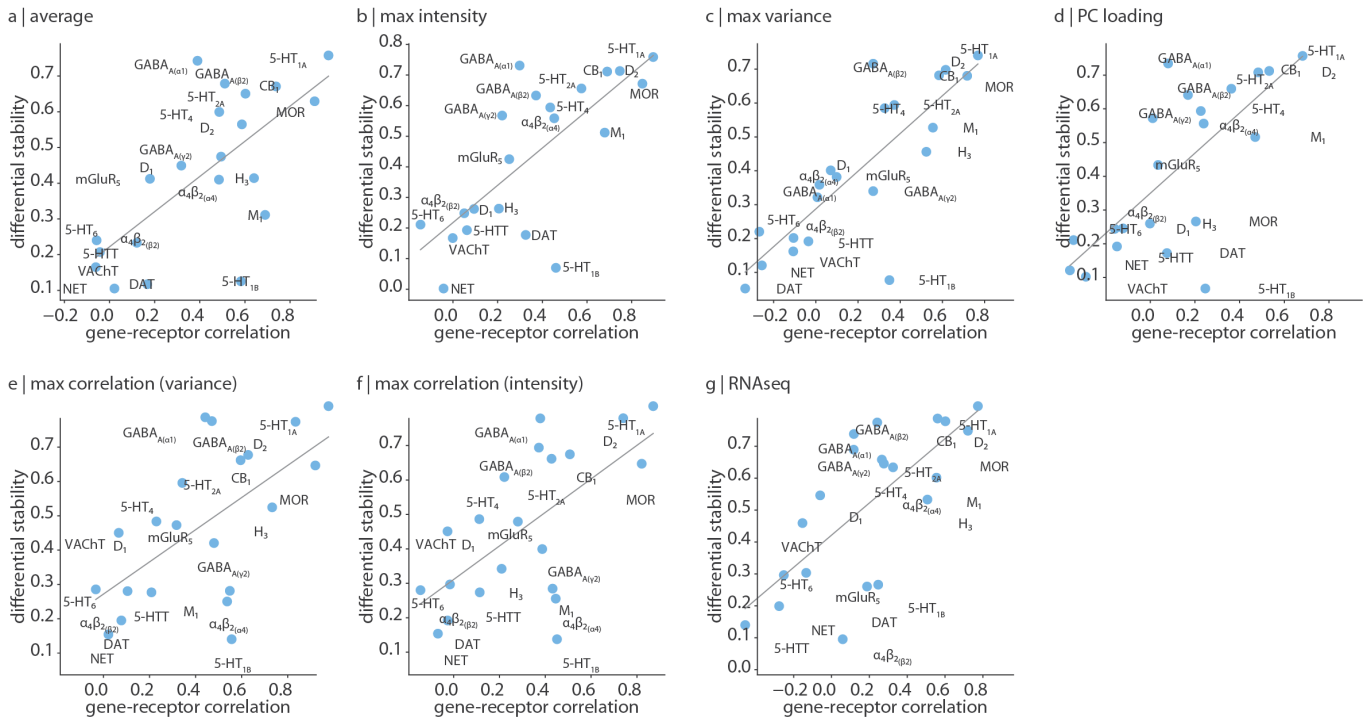
Figure S10. **Comparing probe-selection method |** The relationship between receptor expression-density correspondence and differential stability is conserved when (a) all microarray probes indexing the same gene are averaged together (Spearman $r = 0.55$, $p = 0.009$), (b) the selected probe has maximum average expression (Spearman $r = 0.68$, $p = 0.0007$), (c) the selected probe has maximum variance in expression (Spearman $r = 0.74$, $p = 0.0001$), (d) the selected probe has maximum loading on the first principal component of gene expression (Spearman $r = 0.66$, $p = 0.001$), (e) the selected probe is maximally correlated to other probes from the same gene (if only one probe exists, the maximum variance as in (c) is selected instead; Spearman $r = 0.49$, $p = 0.024$), (f) the selected probe is maximally correlated to other probes from the same gene (if only one probe exists, the maximum intensity as in (b) is selected instead; Spearman $r = 0.55$, $p = 0.010$), and (g) the selected probe has the most consistent pattern of regional variation to RNAseq data (Spearman $r = 0.71$, $p = 0.0003$) [62].
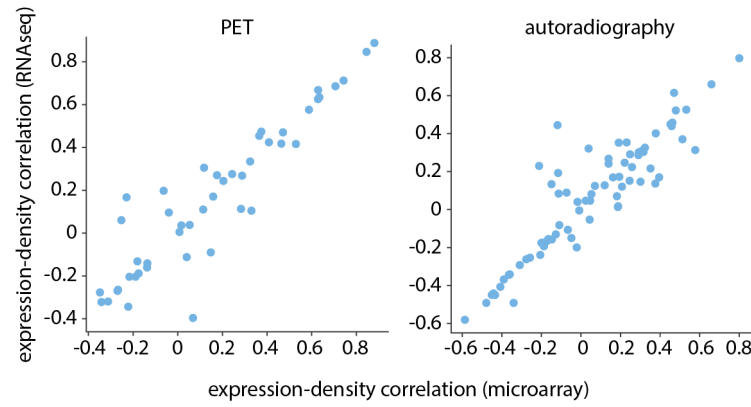
Figure S11. **Microarray versus RNAseq AHBA gene expression |** We plot that expression-density correlation computed for all gene-receptor pairs when calculated using microarray versus RNAseq AHBA gene expression. Each point represents a gene-receptor pair.
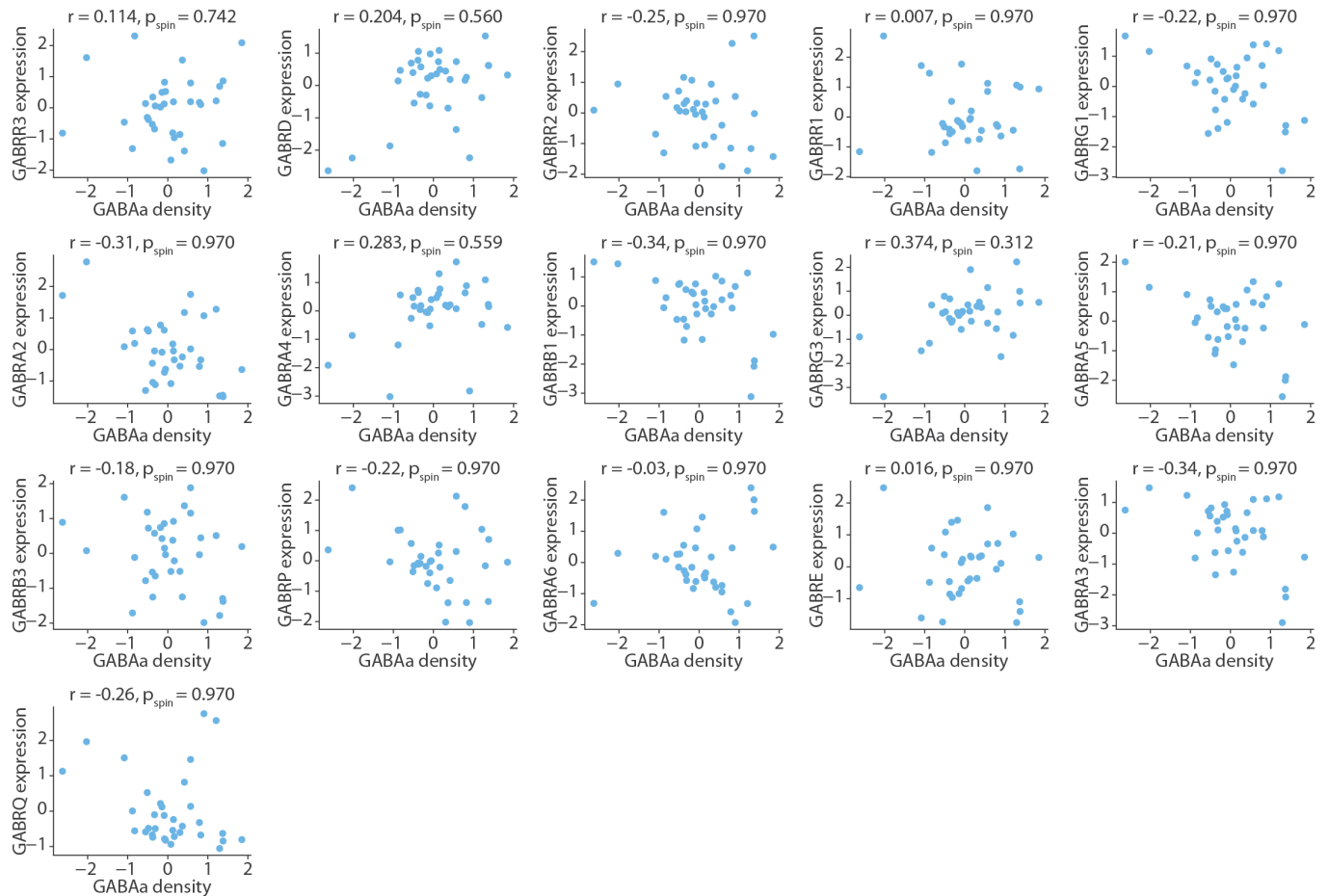
Figure S12. **Expression-density association for the remaining sixteen GABAa subunits |** Expression-density association for the remaining sixteen GABAa subunits that do not comprise the main channel (α_1, β_2, γ_2), after correcting for multiple comparisions (FDR). Receptor density and gene expression is z-scored.

Receptor/transporter	Neurotransmitter	Tracer	Measure	N	Age	References
D_1	dopamine	[^{11}C]SCH23390	BP_{ND}	13	33 ± 13	Kaller et al., 2017 [54]
D_2	dopamine	[^{11}C]FLB-457	BP_{ND}	37	48.4 ± 16.9	Smith et al., 2019 [91, 105]
D_2	dopamine	[^{11}C]FLB-457	BP_{ND}	55	32.5 ± 9.7	Sandiego et al., 2015 [91, 92, 103, 105, 114]
D_2	dopamine	[^{11}C]raclopride	BP_{ND}	7	24 ± 2	Alakurtti et al., 2015 [2]
DAT*	dopamine	[^{123}I]-FP-CIT	SUVR	174	61 ± 11	Dukart et al., 2018 [31]
NET*	norepinephrine	[^{11}C]MRB	BP_{ND}	77	33.4 ± 9.2	Ding et al., 2010 [10, 21, 29, 90]
5-HT$_{1A}$	serotonin	[^{11}C]WAY-100635	BP_{ND}	36	26.3 ± 5.2	Savli et al., 2012 [94]
5-HT$_{1B}$	serotonin	[^{11}C]P943	BP_{ND}	65	33.7 ± 9.7	Gallezot et al., 2010 [6, 39, 66, 71, 72, 82, 93]
5-HT$_{1B}$	serotonin	[^{11}C]P943	BP_{ND}	23	28.7 ± 7.0	Savli et al., 2012 [94]
5-HT$_{2A}$	serotonin	[^{11}C]Cimbi-36	B_{max}	29	22.6 ± 2.7	Beliveau et al., 2017 [11]
5-HT$_4$	serotonin	[^{11}C]SB207145	B_{max}	59	25.9 ± 5.3	Beliveau et al., 2017 [11]
5-HT$_6$	serotonin	[^{11}C]GSK215083	BP_{ND}	30	36.6 ± 9.0	Radhakrishnan et al., 2018 [85, 86]
5-HTT*	serotonin	[^{11}C]DASB	B_{max}	100	25.1 ± 5.8	Beliveau et al., 2017 [11]
$\alpha_4\beta_2$	acetylcholine	[^{18}F]flubatine	V_T	30	33.5 ± 10.7	Hillmer et al., 2016 [5, 48]
M_1	acetylcholine	[^{11}C]LSN3172176	BP_{ND}	24	40.5 ± 11.7	Naganawa et al., 2021 [73]
VAChT*	acetylcholine	[^{18}F]FEOBV	SUVR	4	37 ± 10.2	PI: Lauri Tuominen & Synthia Guimond [44]
VAChT*	acetylcholine	[^{18}F]FEOBV	SUVR	18	66.8 ± 6.8	Aghourian et al., 2017 [1]
VAChT*	acetylcholine	[^{18}F]FEOBV	SUVR	5	68.3 ± 3.1	Bedard et al., 2019 [9]
VAChT*	acetylcholine	[^{18}F]FEOBV	SUVR	3	66.6 ± 0.94	PI: Taylor W. Schmitz & R. Nathan Spreng [44]
mGluR$_5$	glutamate	[^{11}C]ABP688	BP_{ND}	73	19.9 ± 3.04	Smart et al., 2019 [104]
mGluR$_5$	glutamate	[^{11}C]ABP688	BP_{ND}	22	67.9 ± 9.6	PI: Pedro Rosa-Neto [44]
mGluR$_5$	glutamate	[^{11}C]ABP688	BP_{ND}	28	33.1 ± 11.2	DuBois et al., 2016 [30]
GABA$_{A/BZ}$	GABA	[^{11}C]flumazenil	B_{max}	16	26.6 ± 8	Nørgaard et al., 2021 [75]
H_3	histamine	[^{11}C]GSK189254	V_T	8	31.7 ± 9.0	Gallezot et al., 2017 [40]
CB_1	cannabinoid	[^{11}C]OMAR	V_T	77	30.0 ± 8.9	Normandin et al., 2015 [33, 74, 77, 87]
MOR	opioid	[^{11}C]carfentanil	BP_{ND}	204	32.3 ± 10.8	Kantonen et al., 2020 [55]

TABLE S1. **Neurotransmitter receptors and transporters included in analyses** | BP_{ND} = non-displaceable binding potential; V_T = tracer distribution volume; B_{max} = density (pmol/ml) converted from binding potential (5-HT) or distributional volume (GABA) using autoradiography-derived densities; SUVR = standard uptake value ratio. Refer to [44] for more details. Note that [^{11}C]raclopride is used to map subcortical D_2 density while [^{11}C]FLB-457 is used to map cortical D_2 density. Asterisks indicate transporters.

Receptor	Neurotransmitter	Excitatory/Inhibitory	Ionotropic/Metabotropic
AMPA	glutamate	excitatory	ionotropic
NMDA	glutamate	excitatory	ionotropic
Kainate	glutamate	excitatory	ionotropic
GABA$_A$	GABA	inhibitory	ionotropic
GABA$_{A/BZ}$	GABA	inhibitory	ionotropic
GABA$_B$	GABA	inhibitory	metabotropic
M_1	acetylcholine	excitatory	metabotropic
M_2	acetylcholine	inhibitory	metabotropic
M_3	acetylcholine	excitatory	metabotropic
$\alpha_4\beta_2$	acetylcholine	excitatory	ionotropic
α_1	norepinephrine	excitatory	metabotropic
α_2	norepinephrine	inhibitory	metabotropic
5-HT$_{1A}$	serotonin	inhibitory	metabotropic
5-HT$_2$	serotonin	excitatory	metabotropic
D_1	dopamine	excitatory	metabotropic

TABLE S2. **Neurotransmitter receptors included in the autoradiography dataset**

gene	receptor	Spearman r	p_{spin}	gene	receptor	Spearman r	p_{spin}
HTR1A	5HT1a	0.795875	0.009299	GABRG2	GABAa	0.155691	0.805419
HTR1B	5HT1b	0.153247	0.425057	GABRR3	GABAa	0.089381	0.805419
HTR2A	5HT2a	0.166692	0.489651	GABRD	GABAa	0.241864	0.797034
HTR4	5HT4	0.445684	0.099290	GABRR2	GABAa	-0.067991	0.802279
HTR6	5HT6	-0.188999	0.330967	GABRR1	GABAa	-0.101910	0.797034
SLC6A4	5HTT	0.061574	0.722628	GABRG1	GABAa	-0.539190	0.381319
CHRNA2	A4B2	0.053323	0.802520	GABRA2	GABAa	-0.557830	0.381319
CHRNA3	A4B2	-0.267532	0.778172	GABRA4	GABAa	0.131551	0.802279
CHRNA4	A4B2	0.471352	0.558194	GABRB1	GABAa	-0.528801	0.381319
CHRNA5	A4B2	0.365011	0.347565	GABRG3	GABAa	0.423682	0.381319
CHRNA6	A4B2	0.587777	0.152335	GABRA5	GABAa	-0.521772	0.381319
CHRNA7	A4B2	0.288312	0.761564	GABRB3	GABAa	-0.369595	0.414729
CHRNA9	A4B2	-0.175248	0.788621	GABRP	GABAa	-0.460963	0.381319
CHRNA10	A4B2	-0.137357	0.802520	GABRA6	GABAa	0.246448	0.797034
CHRNB2	A4B2	-0.063102	0.802520	GABRE	GABAa	-0.274255	0.778749
CHRNB3	A4B2	0.634530	0.096790	GABRA3	GABAa	-0.416043	0.394738
CHRNB4	A4B2	0.040183	0.802520	GABRQ	GABAa	-0.464629	0.394738
CNR1	CB1	0.742704	0.051995	HRH3	H3	0.628113	0.133387
DRD1	D1	0.138273	0.496950	CHRM1	M1	0.629030	0.001700
DRD2	D2	0.699007	0.038696	GRM5	mGluR5	0.343621	0.118588
SLC6A3	DAT	0.280672	0.185981	OPRM1	MOR	0.802903	0.001800
GABRA1	GABAa	0.245531	0.797034	SLC6A2	NET	-0.136134	0.523948
GABRB2	GABAa	0.525439	0.381319	SLC18A3	VAChT	0.129412	0.473253

TABLE S3. Spearman correlations between microarray gene expression and PET-derived receptor density in the cortex. Significance was assessed against a spatial autocorrelation preserving null model (p_{spin}) and in cases where receptors are repeated, corrected for multiple comparisons [12].

gene	receptor	Spearman r	p	gene	receptor	Spearman r	p
HTR1A	5HT1a	0.950000	3.043129×10^{-08}	GABRG2	GABAa	0.410714	6.416432×10^{-02}
HTR1B	5HT1b	-0.314286	8.730300×10^{-01}	GABRR3	GABAa	-0.253571	8.190919×10^{-01}
HTR2A	5HT2a	0.800000	1.711349×10^{-04}	GABRD	GABAa	0.182143	2.579408×10^{-01}
HTR4	5HT4	0.432143	5.384652×10^{-02}	GABRR2	GABAa	-0.060714	5.850940×10^{-01}
HTR6	5HT6	0.335714	1.106058×10^{-01}	GABRR1	GABAa	-0.564286	9.857837×10^{-01}
SLC6A4	5HTT	-0.146429	6.987250×10^{-01}	GABRG1	GABAa	0.360714	9.327719×10^{-02}
CHRNA2	A4B2	0.639286	5.144223×10^{-03}	GABRA2	GABAa	0.507143	2.683183×10^{-02}
CHRNA3	A4B2	0.425000	5.714774×10^{-02}	GABRA4	GABAa	0.467857	3.931512×10^{-02}
CHRNA4	A4B2	0.592857	9.923211×10^{-03}	GABRB1	GABAa	0.735714	8.849343×10^{-04}
CHRNA5	A4B2	0.342857	1.054619×10^{-01}	GABRG3	GABAa	0.567857	1.361418×10^{-02}
CHRNA6	A4B2	0.350000	1.004727×10^{-01}	GABRA5	GABAa	0.610714	7.796416×10^{-03}
CHRNA7	A4B2	-0.157143	7.120237×10^{-01}	GABRB3	GABAa	0.532143	2.057929×10^{-02}
CHRNA9	A4B2	-0.278571	8.426453×10^{-01}	GABRP	GABAa	-0.150000	7.031849×10^{-01}
CHRNA10	A4B2	-0.575000	9.875319×10^{-01}	GABRA6	GABAa	0.335714	1.106058×10^{-01}
CHRNB2	A4B2	0.032143	4.547311×10^{-01}	GABRE	GABAa	0.200000	2.374070×10^{-01}
CHRNB3	A4B2	-0.075000	6.047446×10^{-01}	GABRA3	GABAa	0.328571	1.159048×10^{-01}
CHRNB4	A4B2	-0.375000	9.157836×10^{-01}	GABRQ	GABAa	0.439286	5.068029×10^{-02}
CNR1	CB1	0.121429	3.332006×10^{-01}	HRH3	H3	0.382143	7.991181×10^{-02}
DRD1	D1	0.867857	1.375903×10^{-05}	CHRM1	M1	0.639286	5.144223×10^{-03}
DRD2	D2	0.842857	3.983598×10^{-05}	GRM5	mGluR5	0.492857	3.097550×10^{-02}
SLC6A3	DAT	-0.396429	9.282527×10^{-01}	OPRM1	MOR	0.621429	6.701003×10^{-03}
GABRA1	GABAa	-0.246429	8.120247×10^{-01}	SLC6A2	NET	0.185714	2.537705×10^{-01}
GABRB2	GABAa	0.067857	4.050544×10^{-01}	SLC18A3	VAChT	0.785714	2.582274×10^{-04}

TABLE S4. Spearman correlations between microarray gene expression and PET-derived receptor density in the subcortex. In cases where receptors are repeated, parametric p-values were corrected for multiple comparisons [12].

gene	receptor	Spearman r	p_{spin}	gene	receptor	Spearman r	p_{spin}
GRIA1	AMPA	0.378166	0.637403	GABRR3	GABAa/BZ	-0.126891	0.865499
GRIA2	AMPA	0.207473	0.637403	GABRD	GABAa/BZ	0.162000	0.943870
GRIA3	AMPA	-0.017220	0.830617	GABRR2	GABAa/BZ	0.190922	0.865499
GRIA4	AMPA	0.300928	0.637403	GABRR1	GABAa/BZ	-0.164674	0.865499
GRIN1	NMDA	-0.276352	0.774923	GABRG1	GABAa/BZ	-0.196272	0.933163
GRIN2A	NMDA	-0.148792	0.774923	GABRA2	GABAa/BZ	-0.309120	0.865499
GRIN2B	NMDA	0.257962	0.774923	GABRA4	GABAa/BZ	0.245925	0.865499
GRIN2C	NMDA	0.139597	0.774923	GABRB1	GABAa/BZ	-0.359609	0.865499
GRIN2D	NMDA	-0.112681	0.774923	GABRG3	GABAa/BZ	0.181894	0.865499
GRIN3A	NMDA	-0.188581	0.774923	GABRA5	GABAa/BZ	-0.478308	0.865499
GRIN3B	NMDA	0.292234	0.774923	GABRB3	GABAa/BZ	-0.364290	0.865499
GRIK1	kainate	0.479478	0.325634	GABRP	GABAa/BZ	-0.211485	0.865499
GRIK2	kainate	0.470785	0.325634	GABRA6	GABAa/BZ	0.395386	0.865499
GRIK3	kainate	0.458246	0.325634	GABRE	GABAa/BZ	-0.146953	0.933163
GRIK4	kainate	0.188080	0.725027	GABRA3	GABAa/BZ	-0.450556	0.865499
GRIK5	kainate	0.309120	0.445080	GABRQ	GABAa/BZ	-0.407256	0.865499
GABRA1	GABAa	0.351584	0.866313	GABBR1	GABAb	0.316141	0.361764
GABRB2	GABAa	0.462259	0.866313	GABBR2	GABAb	0.186408	0.361764
GABRG2	GABAa	0.231046	0.884150	CHRM1	m1	0.043969	0.842216
GABRR3	GABAa	0.119870	0.884150	CHRM2	m2	-0.118365	0.678632
GABRD	GABAa	0.221182	0.884150	CHRM3	m3	0.323497	0.097890
GABRR2	GABAa	0.038786	0.970003	CHRNA2	a4b2	-0.008526	0.999400
GABRR1	GABAa	-0.173034	0.866313	CHRNA3	a4b2	0.046477	0.999400
GABRG1	GABAa	-0.205634	0.884150	CHRNA4	a4b2	0.193931	0.999400
GABRA2	GABAa	-0.340216	0.884150	CHRNA5	a4b2	-0.072557	0.999400
GABRA4	GABAa	0.375993	0.866313	CHRNA6	a4b2	0.532308	0.654985
GABRB1	GABAa	-0.390036	0.884150	CHRNA7	a4b2	-0.066204	0.999400
GABRG3	GABAa	0.577782	0.714329	CHRNA9	a4b2	-0.257628	0.999400
GABRA5	GABAa	-0.434172	0.866313	CHRNA10	a4b2	-0.187077	0.999400
GABRB3	GABAa	-0.199783	0.884150	CHRNB2	a4b2	0.248098	0.999400
GABRP	GABAa	-0.115523	0.884150	CHRNB3	a4b2	0.659701	0.252975
GABRA6	GABAa	0.513082	0.866313	CHRNB4	a4b2	-0.021232	0.999400
GABRE	GABAa	0.024241	0.884150	ADRA1A	a1	0.139597	0.571443
GABRA3	GABAa	-0.586642	0.714329	ADRA2A	a2	0.452562	0.027897
GABRQ	GABAa	-0.442030	0.866313	HTR1A	5-HT1a	0.800301	0.001700
GABRA1	GABAa/BZ	0.052997	0.984302	HTR2A	5-HT2	-0.048316	0.824618
GABRB2	GABAa/BZ	0.290395	0.865499	DRD1	D1	-0.109337	0.801820
GABRG2	GABAa/BZ	0.070551	0.984302				

TABLE S5. Spearman correlations between microarray gene expression and autoradiography-derived receptor density. Significance was assessed against a spatial autocorrelation preserving null model (p_{spin}) and in cases where receptors are repeated, corrected for multiple comparisons [12].

receptor	# AHBA genes	# significant	gene names	# r>0.5
$5HT_{1A}$	18.0	2.0	*HTR2C, HTR1A*	3
$5HT_{1B}$	18.0	0.0		0
$5HT_{2A}$	18.0	0.0		3
$5HT_4$	18.0	3.0	*HTR2C, HTR3B, HTR1A*	4
$5HT_6$	18.0	0.0		0
5HTT	18.0	0.0		0
$\alpha_4\beta_2$	181.0	0.0		18
M_1	181.0	0.0		4
VAChT	181.0	0.0		1
CB_1	26.0	7.0	*GNB2, GNB4, CNR1, CNRIP1, GRM1, GNG4, PLCB2*	10
D_1	71.0	0.0		3
D_2	71.0	0.0		11
DAT	71.0	0.0		2
$GABA_A$	70.0	0.0		2
H_3	62.0	0.0		4
$mGluR_5$	171.0	0.0		0
MOR	47.0	4.0	*ADCY2, GNB2, GNB4, OPRM1*	18
NET	29.0	0.0		2

TABLE S6. **Panther ontology pathways |** For each neurotransmitter receptor, we used the Panther classification system to construct a list of genes related to proteins within the neurotransmitter's protein pathway (using the neurotransmitter's name as a search term, e.g. "dopamine"). Here we show the number of genes in each list, the number and names of genes that are significantly correlated with PET-derived protein density (FDR-correct $p_{spin} < 0.05$), and then number of genes that show large correlation ($r > 0.5$) with PET-derived protein density, irregardless of statistical significance.